Fungal transformation of cedryl acetate and α-glucosidase inhibition assay, quantum mechanical calculations and molecular docking studies of its metabolites

ARTICLE *in* EUROPEAN JOURNAL OF MEDICINAL CHEMISTRY · FEBRUARY 2013

Impact Factor: 3.45 · DOI: 10.1016/j.ejmech.2013.01.036 · Source: PubMed

European Journal of Medicinal Chemistry 62 (2013) 764–770

Contents lists available at SciVerse ScienceDirect

European Journal of Medicinal Chemistry

journal homepage: http://www.elsevier.com/locate/ejmech

Original article

Fungal transformation of cedryl acetate and α-glucosidase inhibition assay, quantum mechanical calculations and molecular docking studies of its metabolites

Sadia Sultan [a,b,*], M. Iqbal Choudhary [a], Shamsun Nahar Khan [a], Urooj Fatima [a], Muhammad Atif [a], Rahat Azhar Ali [d], Atta-ur- Rahman [a], M. Qaiser Fatmi [c,a,d,**]

[a] H.E.J. Research Institute of Chemistry, International Center for Chemical and Biological Sciences, University of Karachi, Karachi, Pakistan
[b] Department of Pharmacology and Chemistry, Atta-ur-Rahman Institute For Natural Product Discovery (RiND), Faculty of Pharmacy, Universiti Teknologi MARA (UiTM), Puncak Alam Campus, 42300 Bandar Puncak Alam, Selangor Darul Ehsan, Malaysia
[c] Department of Biosciences, COMSATS Institute of Information Technology (CIIT), Chak Shahzad, Islamabad, Pakistan
[d] Department of Chemistry, University of Karachi, Karachi, Pakistan

ARTICLE INFO

Article history:
Received 13 July 2012
Received in revised form
29 December 2012
Accepted 29 January 2013
Available online 8 February 2013

Keyword:
Cedryl acetate
Cedrol
Cunninghamella elegans
Human intestinal and pancreatic maltase glucoamylase
α-Glucosidase inhibitory activity
Hartree–Fock (HF) calculations

ABSTRACT

The fungal transformation of cedryl acetate (**1**) was investigated for the first time by using *Cunninghamella elegans*. The metabolites obtained include, 10β-hydroxycedryl acetate (**3**), 2α, 10β-dihydroxycedryl acetate (**4**), 2α-hydroxy-10-oxocedryl acetate (**5**), 3α,10β-dihydroxycedryl acetate (**6**), 3α,10α-dihydroxycedryl acetate (**7**), 10β,14α-dihydroxy cedryl acetate (**8**), 3β,10β-cedr-8(15)-ene-3,10-diol (**9**), and 3α,8β,10β -dihydroxycedrol (**10**). Compounds **1**, **2**, and **4** showed α-glucosidase inhibitory activity, whereby **1** was more potent than the standard inhibitor, acarbose, against yeast α-glucosidase. Detailed docking studies were performed on all experimentally active compounds to study the molecular interaction and binding mode in the active site of the modeled yeast α-glucosidase and human intestinal maltase glucoamylase. All active ligands were found to have greater binding affinity with the yeast α-glucosidase as compared to that of human homolog, the intestinal maltase, by an average value of approximately −1.4 kcal/mol, however, no significant difference was observed in the case of pancreatic amylase.

1. Introduction

It is well known that odoriferous essential oils, which are of high value in the perfume trade, contain some minor constituents which can be regarded as the real odor carriers of these products. This has been demonstrated by the studies carried out on cedrol (**2**), which is a major constituent of essential oils of *Juniperus* species [1]. Cedrol (**2**) possesses a rigid tricyclic sesquiterpene structure and is known to have sedative effects [2]. It is abundantly available as a fragrance or as a synthon for synthesis of related compounds. The microbiological hydroxylation of cedrol (**2**) by *Beauveria* species [3], and *Cephalosporium aphidicola* [4], has been shown to take place predominantly at C(3). Hydroxylations of compound **2** with *Curvularia lunata* [5], *Rhizopus stolonifer* [6], and *Streptomyces bikiniensis* [6] have been less regiospecific, and generally take place at C(2), C(3), C(4), C(9), C(10), and C(12).

The zygomycete fungi of the genus *Cuninghamella* have the ability to metabolize drugs in a manner similar to that in mammals. In the course of our work on microbial transformation of bioactive natural products [7–13], we have studied the transformation of various sesquiterpenes such as (−) ambrox, (+) sclareolide, (+) isolongifolene and (+) isolongifolol [14–16]. In the present study, we have chosen cedryl acetate (**1**), a tricyclic sesquiterpene isolated from the plant *Psidium caudatum* [17], as a model compound and investigated its metabolism by *Cunninghamella elegans* to obtain interesting metabolites with unique structures, as well as to assess the directing role of the acetate group at C(8).

α-Glucosidase inhibitors have been used for the control of blood glucose levels *via* control of the degradation of dietary disaccharides

* Corresponding author. Department of Pharmacology and Chemistry, Atta-ur-Rahman Institute For Natural Product Discovery (RiND), Faculty of Pharmacy, Universiti Teknologi MARA (UiTM), Puncak Alam Campus, 42300 Bandar Puncak Alam, Selangor Darul Ehsan, Malaysia. Tel.: +603 3258 4614, +601 111324812 (mobile); fax: +603 3258 4602.
** Corresponding author. Department of Biosciences, COMSATS Institute of Information Technology (CIIT), Islamabad, Pakistan. Tel.: +92 334 304 3093 (mobile).
E-mail addresses: sadiasultan301@yahoo.com, drsadia@salam.uitm.edu.my (S. Sultan), qaiser.fatmi@comsats.edu.pk (M.Q. Fatmi).

0223-5234/$ – see front matter © 2013 Elsevier Masson SAS. All rights reserved.
http://dx.doi.org/10.1016/j.ejmech.2013.01.036

and starch. Glucosidase inhibitors are valuable in a number of applications such as their use in the study of protein glycosylation and control of viral infections through interference with the, normal glycosylation of viral coat protein [18]. In an ongoing project aimed to develop new α-glucosidase inhibitors, we screened a large number of compounds including cedryl acetate (**1**) and cedrol (**2**). Both exhibited potent α-glucosidase inhibitory activity. Based on this we carried out the microbial transformation of the most potent compound **1**, and screened the transformed products for the same activity. We have reported several α-glucosidase inhibitors more potent than acarbose [19]. However, this is the first report describing the α-glucosidase inhibitory activity of cedrol (**2**), cedryl acetate (**1**), and some of the transformed products of cedryl acetate. The structures have been also optimized computationally at Hartree–Fock (HF) level of theory using valence triple-zeta plus diffuse and polarization functions (6-311++G*) basis sets for H, C, N, and O atoms to get insight into the 3D structure of these metabolites. GAMESS package [20] have been used for all quantum chemical calculations. Molecular docking studies have been also performed to delineate the ligand–protein interactions at molecular level using autodock vina program [21]. Avogadro [22], Gabedit [23], VMD [24] and Chimera [25] have been used for the structure building, analysis and visualization for our calculations.

2. Results and discussion

2.1. Structural elucidations

Cedryl acetate (**1**), $C_{17}H_{28}O_2$, was incubated with *C. elegans* for 6 days to obtain a series of minor metabolites. These metabolites can be divided into two categories. Those retaining the C(8) acetyl group (metabolites **3**–**8**) and those in which deacetylation and then hydration and/or dehydration had taken place (metabolites **2**, **9** and **10**) (Fig. 1).

Compound **3** showed the M+ peak at *m*/*z* 280.1566 ($C_{17}H_{28}O_3$) by HR-EI-MS. The ^{1}H NMR spectrum of **3** showed a new downfield methine signal at δ(H) 3.98, while ^{13}C NMR spectrum also indicated the presence of a new OH-bearing CH C-atom, resonating at δ (C) 71.8. The location of a new OH group at C(10) was deducted on the basis of HMBC interaction of the geminal H-C(10) and C(9) at δ (C) 41.2. Similarly, CH_2(9) (δ (H) 2.18, 2.06) and CH_2(11) (δ (H) 1.93, 1.87) showed HMBC correlations with C(10), further supporting the presence of an OH at C(10). The configuration at the newly created stereogenic center C(10) was deducted by the coupling constant and the NOESY experiment. From these data, the structure of compound 3 was identified as 10β-hydroxycedryl acetate.

The metabolite **4** was isolated as an amorphous solid. The HR-EI-MS of the transformed product **4** revealed the molecular formula $C_{17}H_{28}O_4$ (*m*/*z* 296.2049). The ^{1}H NMR spectrum was also found to be distinctly similar to the compound **3** except that the signal for H-C(12) appeared as a singlet at δ (H) 1.28 (instead of a doublet at δ (H) 0.90, as in compound **3**), while its ^{13}C NMR spectrum displayed a new quaternary C-atom signal (C(2)) at δ (C) 80.0 (Table 1). This was also inferred from HMBC correlations of CH2(3) (δ (H) 2.50, 2.24) and H-C(12) (δ (H) 1.28) with C(2) at δ (C) 80.0. A downfield doublet at δ (H) 4.05 (*J*(10eq,9ax) = 4.9), correlated with a CH C-atom signal at δ 72.2 in the HMQC spectrum, indicating the presence of another OH group at C(10), as was observed in compound **3**. The configuration of the stereogenic center C(10) was found to be (*R*), same as in metabolite **3.** On the basis of these spectral data, compound **4** was identified as 2α,10β-dihydroxycedryl acetate.

The HR-EI-MS of **5** showed the M+ at *m*/*z* 294.1862 ($C_{17}H_{28}O_4$), indicating two additional O-atoms, as compared to substrate **1**. Its ^{13}C NMR spectra also displayed two additional quaternary C-atom signals at δ (C) 78.0 and 210.2, indicating the presence of OH and C=O functionalities. The position of the C(10)=O was deducted on the basis of HMBC correlations of CH2 (9) (δ (H) 2.94, 2.75) and CH2(11) (δ (H) 2.38, 1.52) with C(10) at δ (C) 210.2. The newly introduced OH group was placed at C(2) (δ 78.0) on the basis of chemical-shift comparison with the compound **4**. From these spectral data, metabolite **5,** 2α-hydroxy-10-oxocedryl acetate, was found to be a C(10)-oxidized derivative of metabolite **4**.

The HR-EI-MS of compound **6** showed the M+ at *m*/*z* 296.2090 ($C_{17}H_{28}O_4$), indicating two additional O-atoms as compared to **1**. The ^{1}H NMR spectrum showed two new CH signals at δ (H) 3.84 (d, *J*(10eq, 9ax) = 4.9) and 3.70 (dt, *J* (3β, 4α) = 13.6, *J* (3β, 2α) = 13.6, *J* (3β, 4β) = 7.6). The ^{13}C NMR spectrum of **6** (Table 1) showed additional methine signals at δ (C) 72.0 and 81.4, suggesting the hydroxylation at C(10) and C(3), respectively. The HMBC spectrum showed heteronuclear interactions between H-C(3), and C(2) and C(12) resonating at δ (C) 49.1 and 14.0, respectively; and between H-C(10), and C(8), C(9), and C(15), resonating at δ (C) 86.0, 35.3, and

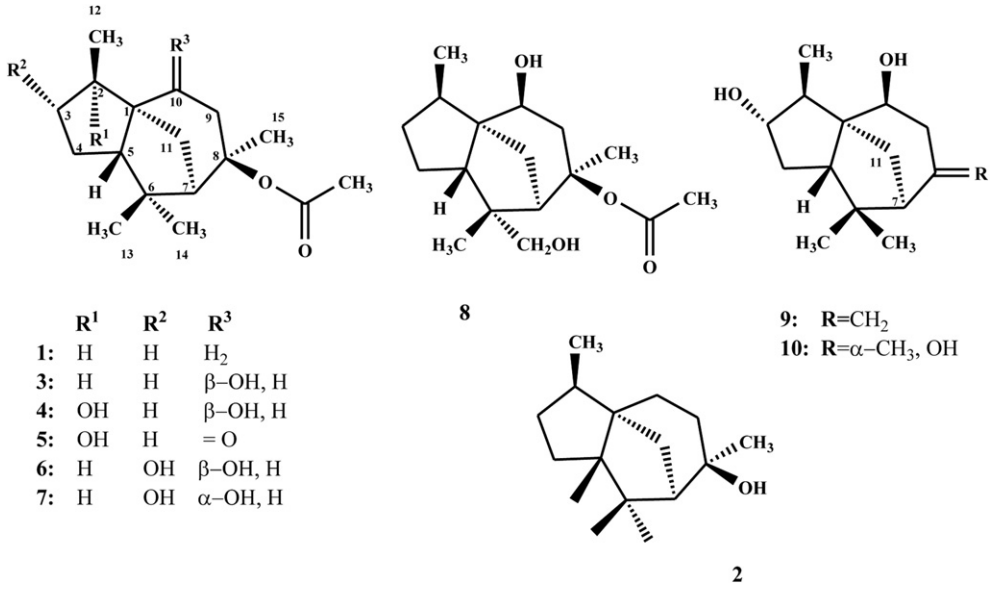

Fig. 1. Structure of cedryl acetate and its derivatives

Table 1
^{13}C NMR data for compounds **1**–**10.**

No.	1	2	3	4	5	6	7	8	9	10
1	55.0	54.4	60.0	60.3	60.0	56.8	55.2	60.2	59.2	64.8
2	40.0	41.1	37.8	80.0	78.0	49.1	49.4	37.6	50.0	49. 0
3	38.0	37.0	34.2	39.7	38.8	81.1	81.5	33.2	81.5	81.2
4	24.0	25.3	24.0	21.4	21.3	34.1	35.3	29.6	34.9	34.4
5	56.2	56.6	56.0	55.1	52.7	53.1	53.9	50.0	52.4	61.3
6	43.8	43.4	44.1	44.7	45.8	38.0	42.6	67.5	42.0	22.6
7	54.0	61.0	53.8	52.3	54.8	57.3	59.5	53.9	60.3	52.4
8	86.0	75.3	85.9	85.8	85.6	86.0	92.0	85.0	147.8	74.2
9	41.0	35.3	41.2	41.6	52.5	35.3	41.0	41.5	39.0	40.4
10	34.2	31.6	71.8	72.2	210.0	72.0	70. 0	71.4	71.8	72.4
11	31.2	42.0	33.6	30.0	37.0	40.0	29.3	40.4	38.4	29.7
12	15.4	15.6	15.3	23.5	25.0	14.0	25.7	15.4	13.8	13.6
13	27.8	27.6	28.0	28.1	28.3	29.5	25.1	69.7	27.7	30.1
14	28.2	28.9	28.4	28.2	28.1	28.0	27.1	23.2	26.5	28.7
15	27.2	30.2	27.4	27.5	26.4	27.2	25.9	27.5	110.5	13.6
OAc	22.5	–	32.3	22.7	22.4	22.9	22.5	22.5	_	_
	170.1	–	170.2	170.1	171.1	170.2	171.1	170.2		

27.2, respectively, further indicating the location of the additional OH groups. The configurations at the newly created stereogenic centers C(3) and C(10) were deducted by NOESY experiments. From these spectral data, the structure of metabolite **6** was identified as 3α,10β-dihydroxycedryl acetate.

The HR-EI-MS of the compound **7** exhibited the M+ at *m*/*z* 296.1919 ($C_{17}H_{28}O_4$,). The ^{1}H NMR spectrum showed two downfield signals for CH H-atoms geminal to two OH groups at δ (H) 3.64 (*dt*, *J*(3β, 4α) = 13.0, *J*(3β, 2α) = 13.0, *J*(3β, 4β) = 7.5) and 4.16 (*dd*, *J*(10*ax*, 9*ax*) = 10.5, *J* (10*ax*, 9*eq*) = 7.1). The ^{13}C NMR spectra of the compound **7** also showed two CH C-atom signals at δ (C) 70.0 and 81.5. The locations of the two OH groups were found to be same as in metabolite **6** on the basis of 2D-NMR spectrum. The configuration at C(3) and C(10) were inferred through chemical shifts and NOESY interactions, and compound **7** was identified as 3α,10α-dihydroxycedryl acetate.

Further hydroxylation of compound **3** yielded compound **8**. The HR-EI-MS of **8** exhibited the M+ peak at *m*/*z* 296.1984 ($C_{17}H_{28}O_4$). The ^{1}H NMR spectrum displayed the absence of a Me-group signal and the appearance of CH2OH signals as *AB*-type doublets at δ (H) 3.43 and 3.56 (*J* = 10.6 Hz), and δ (C) 69.9. The location of the OH group at C(13) was deducted on the basis of HMBC correlations of CH2(13) (δ (H) 3.43/3.56) with C(5), C(6), and C(14) at δ (C) 50.0, 48.9, and 23.2, respectively. The location was further deduced on the basis of a NOESY experiments. The structure of the metabolite **8** was deduced as 10β,14α-dihydrooxycedryl acetate.

Metabolite **9** was isolated as a white powder. The HR-EI-MS showed the M+ peak at *m*/*z* 236.1786, corresponding to the molecular formula $C_{15}H_{24}O_2$. The ^{1}H NMR spectrum of compound **9** indicated the absence of both Me groups at C(15) and C(17), indicating deacetylation of compound **6**. It also displayed two broad singlets at δ (H) 4.64 and 4.66, which were ascribed to the exocyclic olefinic H-atoms at C(15). The ^{13}C NMR spectra displayed additional olefinic carbon signals at δ (C) 147.8 and 110.5, assigned to C(8) and C(15), respectively. The ^{13}C NMR spectrum also showed two CH C-atoms resonating at δ (C) 81.5 and 71.8, suggesting the presence of OH groups at C(3) and C(10), respectively. The HMBC couplings of the H-C(7) (δ (H) 2.26) and CH2(11) (δ (H) 2.01, 1.75) with C(8) (δ (C) 147.8) also supported a C=C bond between C(8) and C(15). The configurations at the newly created stereogenic centers C(3) and C(10) were deduced by a NOESY experiment. From these spectral data, the structure of metabolite **9** was deduced as 3β,10β-cedr-8(15)-ene-3,10-diol.

The HR-EI-MS of compound **10** showed the M+ peak at *m*/*z* 254.1872, corresponding to the formula $C_{15}H_{26}O_3$. The absence of ester moiety in IR spectrum, indicated the deacetylation at C(8). The location and configuration of the OH groups were found to be the same as for compound **6**, on the basis of the comparison of the spectral data. Compound **10** was deduced to be the deacetylated derivative of compound **6**, and identified as 3α,10β-dihydroxycedrol.

2.2. Biological activity

Compounds **1**, **2**, **4,** and **6** were tested for inhibition of the α-glucosidase enzyme by the method described in Section 3. The α-glucosidase inhibitory activity of the cedrol (**2**) and cedryl acetate (**1**) has been reported here for the first time. According to the results, the cedryl acetate (**1**) showed more inhibitory effect than the cedrol (**2**) which may be due to the presence of an Ac group at C(8). Overall compounds **1, 2,** and **4** showed more than or comparable activity to the standard inhibitors (Table 2). Apparently, the polar OH group lowers the inhibitory activity towards the enzyme, as observed in compounds **4** and **6** (inactive) in comparison to **1**. Compounds **3, 5,** and **7**–**10** were not tested due to insufficient quantities after spectroscopic analysis.

2.3. Geometry optimization

The biological activity of ligands is a function of their 3D structures, therefore, a correct description of the ligand in 3D space is very critical. The structural details of all metabolites have been probed through the geometry optimization in the gaseous-phase using Hartree–Fock approach with valence triple-zeta plus diffuse and polarization functions (6-311++G*) basis sets. The bond distance between C and OH is 1.421 Å in all compounds. The optimized geometry shows the length of carbonyl groups (C=O and COC=OCH_3) to be the shortest one with a distance of 1.208 Å in all compounds, however, the bond order is slightly higher by a value of 0.11 in the case of C=O as expected. The carbon–oxygen bond in C-O$COCH_3$ is slightly larger as compared to that in CO-$COCH_3$ (1.402 Å and 1.338 Å, respectively) due to a lower bond order by a value of 0.233. The presence of acetate group (–O–CO–CH_3) in the molecule lowers the dipole moment of the molecule as could be seen in Table 3. Due to limited experimental inhibitory assay data it is not possible to generalize this observation, nonetheless, among the studied compounds a molecule with low dipole moment seems to be the most active one.

2.4. Molecular docking

The preferred orientation of ligands in 3D space into the protein binding site determines the activity of that ligand, therefore, the ligand–protein binding modes and interactions are very crucial to understand the catalytic activity. Since, the 3D structure of yeast

Table 2
α-Glucosidase inhibitory activity of compounds **1**, **2**, **4** and **6** with their predicted binding energies in the active sites of yeast and mammalian α-glucosidases.

Compounds	IC50[a] (in mM ± S.E.M.)	Binding energy in kcal/mol (yeast α-glucosidase)	Binding energy in kcal/mol (human intestinal maltase glucoamylase)		Binding energy in kcal/mol (human pancreatic amylase; 1U33.pdb)
			C-terminal domain (3TOP.pdb)	N-terminal domain (3L4T.pdb)	
1	94 ± 15	−8.4	−6.9	−6.5	−7.9
2	130 ± 15	−7.4	−6.6	−6.2	−7.9
4	690 ± 16	−7.9	−6.3	−7.1	−7.6
6	Inactive	−8.2	−6.4	−6.5	−7.6
Acarbose	780 ± 20	–	–	–	–
Deoxynojirimycin	425.6 ± 8.14	–	–	–	–

Metabolites **3**, **5** and **7**–**10** could not be screened because of their insufficient quantities.
[a] *IC 50* values are the 'mean ± standard error mean (S.E.M.)' of three assays.

α-glucosidase has not yet been determined by any experimental methods, we took the 3D coordinates of the modeled yeast α-glucosidase from one of our recent studies to be in compliance with the performed bioassay experiments. This modeled protein has been used as our target protein. Additionally, we also performed molecular docking studies of active compounds with the human intestinal and pancreatic maltase glucoamylase to verify their bindings with mammalian α-glucosidase. No significant difference in the binding affinity of active ligands with yeast α-glucosidase and human pancreatic maltase glucoamylase was observed. However, some differences in the binding energy were observed when ligands bind with the human intestinal maltase (Table 2). This less affinity of ligands towards intestinal maltase as compared to the yeast α-glucosidase can be attributed to the structural changes in the binding sites of these proteins. Fig. 2a shows the homology model of the yeast α-glucosidase with the ligand cluster into the binding site. Fig. 2b displays the close view of the binding site with the best predicted orientation of ligands **1**–**15,** obtained from the molecular docking studies, almost overlapping with each other to form a cluster. The amino acid residues forming the binding site cavity have been labeled in white. The cavity can be clearly visualized when the protein is shown with surface model as depicted in Fig. 2c.

Fig. 3 displays the interactions of individual metabolites **1, 2, 4** and **6** with the yeast α-glucosidase protein. Polar amino acid residues *i.e*. Asp349 and Arg439 have strong H-bonding with the acetate group of the ligand. Cedryl acetate (**1**) exhibits the strongest binding affinity with the protein as inferred by its lowest binding energy (−8.4 kcal/mol), the values are given in Table 2. This observation is in good agreement with the enzymatic assay where the compound **1** shows the lowest IC_{50} value (94 ± 15 μM). The metabolite **2**, where the acetate group has been hydrolyzed to the hydroxyl group, does not show any interaction with those residues. These missing interactions (Fig. 3b) may have a partial role in its decreased activity as compared to the compound **1**. On the other hand, metabolites **4** and **6** are acetylated and they do form H-bonds with Asp349 and Arg439, thereby showing a good ligand−protein binding energy, however, their activity is dramatically lowered or diminished as compared to compound **1**. This attenuate activity of metabolites **4** and **6** may be associated with their high polarity arising from the introduction of two hydroxyl groups into the rings, partially due to the fact that the neighboring residues around −OH are slightly hydrophobic in nature.

Table 3
Dipole moment of metabolites calculated at HF/6-311++G* level of theory and basis sets.

Compound	Dipole (Debye)
1	2.03
2	3.03
3	2.87
4	3.87
5	5.07
6	3.90
7	4.09
8	3.93
9	2.65
10	6.01

3. Experimental part

3.1. General

Cedryl acetate (**1**) was purchased from Fluka. Column chromatography (CC): silica gel (70–230 mesh). TLC: silica gel protected *PF254* plates (0.25 mm; Merck); detection by spraying with vanillin soln. M.P.: Büchi-535 apparatus; uncorrected. Optical rotations: JASCO DIP-360 digital polarimeter; in $CHCl_3$. UV spectra: Hitachi U-3200 spectrophotometer; λ_{max} in nm. IR spectra: Shimadzu FT-IR-8900 spectrophotmeter; in cm^{-1}. ^1H NMR and ^{13}C NMR spectra: Bruker Avance-400 apparatus, at 500 (^1H) and 125 MHz (^{13}C), respectively, in $CDCl_3$ solution; chemical shifts δ in ppm. rel to Me_4Si as internal standard, coupling constant *J* in Hz. EI- and HR-EI-MS: Jeol JMS-600 II mass spectrometer; in *m*/*z* (rel.%).

3.2. Organism and culture media

Fungal culture of *C. elegans* (TSY-0865) was grown on Sabouraud-4% glucose agar (Merck) at 25°, and stored at 4 °C. The medium was prepared by mixing the following ingredients in distilled H_2O (4.0 l): glucose (40.0 g), glycerol (40.0 g), peptone (20.0 g), KH_2PO_4 (20.0 g), yeast extract (20.0 g) and NaCl (20.0 g).

3.3. Fermentation

The fungal media was transferred into conical flasks (100 ml each) and autoclaved at 121 °C. Fermentation was carried out according to a standard two-stage protocol [26]. Cedryl acetate (**1**) (800 mg) in acetone (20 ml) was evenly distributed among the 40 flasks (20 mg/0.5 ml in each flask), containing 24-h-old stage-II culture. Fermentation was carried out for 6 days on a rotary shaker (200 rpm) at 25 °C. For analysis, the content of each flask was analyzed by TLC every 2 days. In all experiments, one control flask without fungus (for checking substrate stability) and other flask without exogenous substrate (for checking endogenous metabolite) were used.

3.4. Compound isolation

The culture media and mycelium were separated by filtration. The mycelium was washed with CH_2Cl_2 (3 l), and the filtrate was extracted with CH_2Cl_2 (16 l). The combined organic extracts were

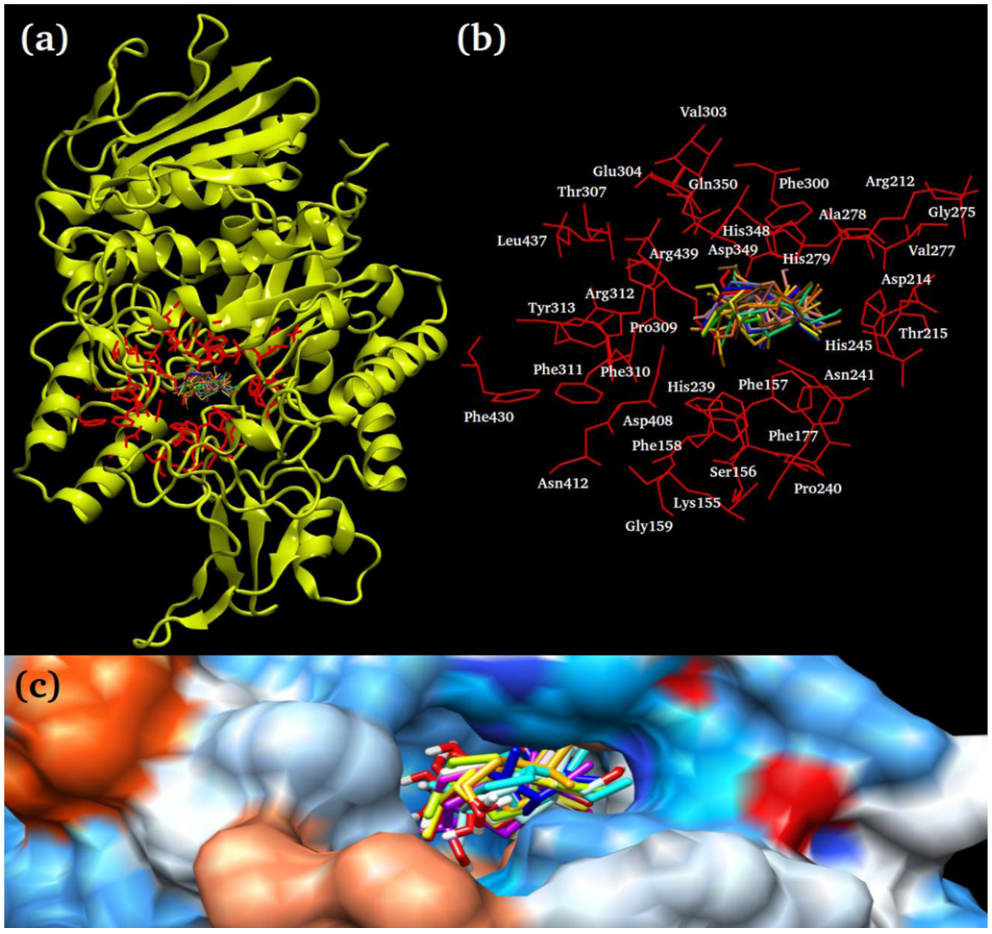

Fig. 2. (a) Homology model of the yeast α-glucosidase (yellow color) showing the ligand cluster (variable color; licorice) into the binding site. The red color indicates the amino acid residues (labeled in white) surrounding the binding site (b). The lower picture (c) displays the binding site cavity with the ligand cluster. (For interpretation of the references to color in this figure legend, the reader is referred to the web version of this article.)

dried (Na_2SO_4), evaporated under reduced pressure, and analyzed by TLC. The control flaks were also harvested and compared with the test by TLC to confirm the presence of the metabolites. The resulting brown gummy extract (1.59 g) was purified using repeated CC (silica gel; petroleum ether (PE)/AcOEt gradient). Elution with 7% AcOEt in PE afforded **3** (3.7 mg), and further elution yielded **4** (11.6 mg; PE/AcOEt 82:18), **5** (2.7 mg; PE/AcOEt 80:20), **6** (16.4 mg; PE/AcOEt 80:20), **7** (3.6 mg; PE/AcOEt 79:21), **8** (2.9 mg; PE/AcOEt 75:25), **9** (2.7 mg; PE/AcOEt 65:35), and **10** (3.3 mg; PE/AcOEt 62:38).

3.4.1. 10β-Hydroxycedryl acetate (**3**)

Gummy, $[\alpha]_{25D} = +64.2$ ($c = 0.02$, $CHCl_3$). IR ($CHCl_3$) ν_{max} cm^{-1}: 3458, 2923, 1728. ^1H NMR ($CDCl_3$, 500 MHz) δ: 3.98 (1H, d, J (10α, 9β) = 4.6 Hz, H-10), 2.18 (1H, brd, J 9(a—b) = 14.8 H-9a), 2.06 (1H, dd, J 9(a—b) = 14.8 Hz, J 9β, 10α = 4.6 Hz, H-9b), 1.93 (1H, m, H-11a), 1.87 (1H, m, H-11b), 1.78 (1H, d, J (7, 11) = 4.9 Hz, H-7), 1.71 (3H, s, CH_3-15), 1.48 (1H, m, H-4a), 1.40 (1H, m, H-4b), 0.90 (3H, d, $J_{(2,12)}$ = 7.0 Hz, CH_3-12), 1.0 (3H, s, CH3-13), 1.12 (3H, s, CH_3-14), 1.92 (3H, s, OAc). ^{13}C NMR δ ($CDCl_3$, 100 MHz): Table 1. EI-MS m/z (rel. int. %): 280 [M+] (29), 294 (4), 143 (16), 122 (100), 121 (88), 91(70), 55 (27), 53 (18); HR-EI-MS: m/z 280.1566 (calc. 280.1596 for $C_{17}H_{28}O_3$).

3.4.2. 2α,10β-Dihydroxycedryl acetate (**4**)

Gummy, $[\alpha]_{25D} = +42.4$ ($c = 0.04$, $CHCl_3$). IR ($CHCl_3$) ν_{max} cm^{-1}: 3423, 1724: ^1H NMR ($CDCl_3$, 400 MHz) δ 4.05 (1H, d, J (10α, 9β) = 4.9 Hz, H-10), 2.21 (1H, m, H-9a), 2.17 (1H, m, H-11a), 1.98 (1H, m, H-9b), 1.74 (3H, s, CH_3-15), 1.66 (1H, m, H-7), 1.28 (3H, s, CH_3-12), 1.04 (3H, s, CH_3-13), 1.10 (3H, s, CH_3-14), 1.74 (3H, s, CH_3-15), 1.92 (3H, s, OAc). ^{13}C NMR ($CDCl_3$, 100 MHz): δ see Table 1. EI-MS m/z (rel. int. %): 296 [M+] (29), 294 (4), 143 (16), 122 (100), 121 (88), 91(70), 55 (27), 53 (18). HR-EI-MS: m/z 296.2049 (calc. 296.2077 for $C_{17}H_{28}O4$).

3.4.3. 2α-Hydroxy-10-oxocedryl acetate (**5**)

Gummy. $[\alpha]_{25D} = +74$ ($c = 0.02$, $CHCl_3$). IR ($CHCl_3$) ν_{max} cm^{-1}: 3442, 1706. ^1H NMR ($CDCl_3$, 400 MHz): δ 2.94 (1H, d, J = 13.6 Hz, H-9a), 2.75 (1H, d, J 9(a—b) = 13.6 Hz, H-9a), 2.67 (1H, d, J (7, 11) = 4.5 Hz, H-7), 2.38 (1H, dd, J 11 (a—b) = 14.1 Hz, J (11, 7) = 4.9 Hz, H-11a), 1.91 (1H, m, H-4a), 1.53 (3H, s, CH_3-15), 1.52 (1H, m, H-11b), 1.46 (3H, s, CH_3-12), 1.40 (1H, m, H-4b), 1.30 (3H, s, CH_3-13), 1.25 (3H, s, CH_3-14), 1.53 (3H, s, CH_3-15), 1.97 (3H, s, OAc). ^{13}C NMR ($CDCl_3$, 100 MHz): δ see Table 1. EI-MS m/z (rel. int. %): 294 [M+] (4), 276 [M+−18] (4), 176.0 (100), 122 (35), 107 (64), 91 (39), 69 (53), 55 (76). HR-EI-MS: m/z 294.1872 (calc. 294.1830 for $C_{17}H_{26}O_4$).

3.4.4. 3α,10β-Dihydroxycedryl acetate (**6**)

Gummy, $[\alpha]_{25D} = +14.2$ ($c = 0.02$, $CHCl_3$). IR ($CHCl_3$) ν_{max} cm^{-1}: 3428, 1710. ^1H NMR ($CDCl_3$, 400 MHz): δ 3.84 (1H, d, J 10α, 9β = 4.9 Hz, H-10), 3.70 (1H, dt, J (3β, 4β) = 13.6 Hz, J (3β, 2α) = 7.6 Hz, H-3β), 2.36 (1H, d, J (7, 11) = 4.9 Hz, H-7), 2.18 (1H, m, H-11a), 2.05 (1H, m, H-11b), 1.89 (1H, m, H-4a), 1.78 (1H, m, H-9a), 1.72 (3H, s, CH_3-15), 1.68 (1H, m, H-5), 1.54 (1H, m, H-2α), 1.48 (1H, m, H-4b), 1.07 (3H, d, $J_{(2, 12)}$ = 7.5 Hz, CH_3-12), 1.05 (3H, s, CH_3-13), 1.15 (3H, s, CH_3-14), 1.92 (3H, s, OAc). ^{13}C NMR ($CDCl_3$, 100 MHz): δ see Table 1.

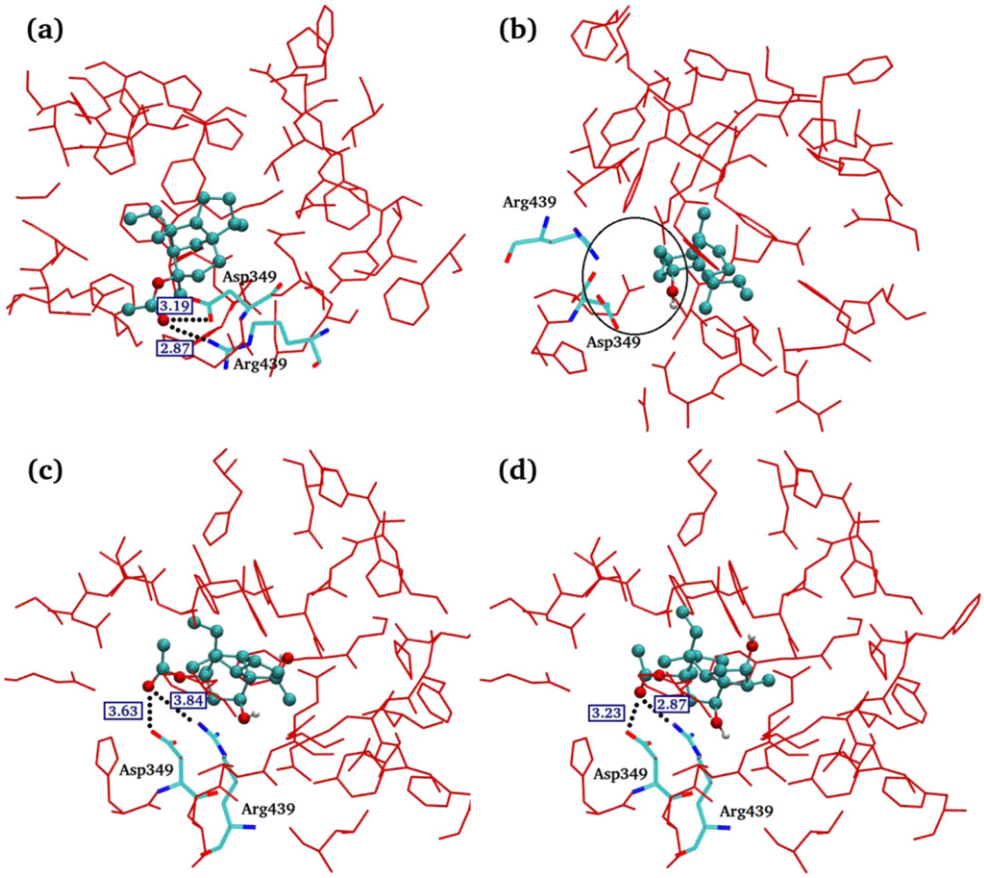

Fig. 3. Ligand–protein interaction studies of compounds (a) **1**, (b) **2**, (c) **4** and (d) **6**. The hydrogen bonds are shown as black dotted lines. The H-bond distances in Å are given in boxes. The amino acid residues in the binding pockets are indicated as red. (For interpretation of the references to color in this figure legend, the reader is referred to the web version of this article.)

EI-MS *m/z* (rel. int. %) 296 [M+] (29), 264 (3), 236 (100), 218 (50), 91 (7), 55 (25), HR-EI-MS *m/z* 296.2090 (calc. 296.2065 for $C_{17}H_{28}O_4$).

3.4.5. 3α,10α-Dihydroxycedryl acetate (*7*)

Gummy, $[\alpha]_{25D} = +56.8$ ($c = 0.03$, $CHCl_3$). IR ($CHCl_3$) ν_{max} cm^{-1}: 3458, 1728. ^1H NMR ($CDCl_3$, 400 MHz): δ 4.16 (1H, dd, J (10β, 9β) = 10.5 Hz, J (10β, 9α) = 7.1 Hz, H-10), 3.64 (1H, dt, J (3β, 4β) = 10.0 Hz, J (3β, 2α) = 4.9 Hz, H-3), 1.86 (1H, m, H-9a), 1.85 (1H, m, H-4a), 1.58 (1H, m, H-4b), 1.52 (1H, m, H-2), 1.41 (3H, s, CH3-15), 1.28 (1H, m, H-9b), 1.23 (1H, m, H-11a), 1.15 (1H, s, CH3-13), 1.01 (1H, s, CH3-14), 0.90 (3H, d, $J_{(2,\ 12)}$ = 7.0 Hz, CH_3-12). 1.01 (3H, s, CH_3-14), 1.97 (3H, s, OAc). ^{13}C NMR ($CDCl_3$, 100 MHz): δ see Table 1. EI-MS *m/z* (rel. int. %) 296 [M+] (29), 294 (4), 143 (16), 122 (100), 121 (88), 91(70), 55 (27), 53 (18). HR-EI-MS *m/z* 296.1919 (calc. 296.1987 for $C_{17}H_{28}O_4$).

3.4.6. 10β,14α–Dihydroxycedryl acetate (*8*)

Gummy, $[\alpha]_{25D} = +51$ ($c = 0.06$ $CHCl_3$). IR ($CHCl_3$) ν_{max} cm^{-1}: 3458, 1728. ^1H NMR ($CDCl_3$, 400 MHz): δ 3.96 (1H, d, J (10α, 9β) = 4.7 Hz, H-10), 3.56 (1H, d, J (a–b) = 10.6 Hz, H14a), 3.43 (1H, d, J (b–a) = 10.6 Hz, H14b), 2.24 (1H, m, H-11a), 2.05 (1H, m, H-9a), 1.64 (1H, m, H-7), 1.56 (1H, m, H-2), 1.38 (1H, m, H-4a), 1.27 (3H, s, H-15),1.22 (1H, m, H-4b), 1.21 (1H, s, CH_3-13), 0.90 (3H, d, J (2, 12) = 7.1 Hz, CH_3-12). ^{13}C NMR ($CDCl_3$, 100 MHz): δ see Table 1. EI-MS *m/z* (rel. int.%): 296 [M+] (4), 280 (6), 236 (23), 218 (90), 55 (33). HR-EI-MS: *m/z* 296.1984 (calc. 296.1904 for $C_{17}H_{28}O_4$).

3.4.7. 3β,10β-Dihydroxycedr-8(15)-ene (*9*)

Gummy, $[\alpha]_{25D} = +44.2$ ($c = 0.02$, $CHCl_3$). IR ($CHCl_3$) ν_{max} cm^{-1}: 3432, 1726. ^1H NMR ($CDCl_3$, 400 MHz): δ 4.66 (1H, s, H-15b), 4.64 (1H, s, H-15a), 3.81 (1H, d, J (10α, 9β) = 3.6 Hz, H-10), 3.70 (1H, dt, J (3β, 2α) = 13.3 Hz, J (3β, 2α) = 8.0 Hz, H-3), 2.58 (1H, d, J 9(a–b) = 16.3 Hz, H-9a), 2.26 (1H, m, H-7), 2.13 (1H, d, J = 16.5 Hz, m, H-9b), 2.00 (1H, m, H-11a), 1.88 (1H, d, J = 11.8 Hz, H-4a), 1.75 (1H, m, H-11), 1.73 (1H, m, H-5), 1.56 (1H, m, H-2), 1.50 (1H, m, H-4b), 1.10 (3H, d, $J_{(2,12)}$ = 7.2 Hz, CH_3-12), 1.03 (1H, s, CH_3-13), 0.94 (1H, s, CH_3-14). ^{13}C NMR ($CDCl_3$, 100 MHz): δ see Table 1. EI-MS *m/z* (rel. int. %): 236 [M+] (100), 218 (100), 200 (75), 162 (49), 157 (60), 148(40), 121 (98), 91 (92); 55 (41). HR-EI-MS *m/z* 236.1786 (calc. 236.1776 for $C_{15}H_{24}O_2$).

3.4.8. 3α,8β,10β-Trihydroxycedrol (*10*)

Gummy, $[\alpha]_{25D} = +24$ ($c = 0.03$, $CHCl_3$). IR ($CHCl_3$) ν_{max} cm^{-1}: 3432, 1726. ^1H NMR ($CDCl_3$, 400 MHz): δ 3.78 (1H, d, J(10α, 9β) = 4.6 Hz, H-10), 3.64 (1H, dt, J(3β, 4β) = 8.5 Hz, J (3β, 2α) = 5.4 Hz, H-3), 2.51 (1H, d, J(3β, 4β) = 8.2 Hz, H-4), 1.56 (1H, m, H-2), 1.97 (1H, m, H-9a), 1.67 (1H, m, H-9b), 1.64 (1H, m, H-7), 1.27 (3H, s, CH3-15), 1.12 (1H, m, H-11a), 1.09 (3H, d, $J_{(2,12)}$ = 7.3 Hz CH_3-12), 1.08 (1H, s, CH_3-13), 1.12 (1H, s, CH_3-14). ^{13}C NMR ($CDCl_3$, 100 MHz): δ see Table 1. EI-MS *m/z* (rel. int. %): 254 [M+] (29), 236 [M+−18] (23), 218 (12), 201 (100), 147 (45), 121 (59), 107 (51), 55 (53), 53 (18). HR-EI-MS: *m/z* 254.1893 (calc. 254.1927 for $C_{15}H_{26}O_3$).

3.5. α-Glucosidase inhibition assay

α-Glucosidase (E.C.3.2.1.20) enzyme inhibition assays were performed according to the slightly modified method of [27]. α-Glucosidase (E.C.3.2.1.20) from *Saccharomyces* sp. was purchased from Wako Pure Chemical Industries Ltd. (Wako 076-02841). The

inhibitions were measured spectrophotometrically at pH 6.9 and at 37 °C using 0.7 mM *p*-nitrophenyl α-D-glucopyranoside (PNP-G) as a substrate and 250 m units/mL enzyme, in 50 mM sodium phosphate buffer containing 100 mM NaCl. 1-Deoxynojirimycin (0.425 mM) and acarbose (0.78 mM) were used as positive controls. The increment in absorption at 400 nm due to the hydrolysis of PNP-G by α-glucosidase was monitored continuously with the help of a spectrophotometer (Spectra Max Molecular Devices, USA).

Acknowledgments

We are grateful to Higher Education Commission, Islamabad, Pakistan, 600-RMI/ERGS 5/3 (4/2012) and Dana Kecemerlangan 600-RMI/DANA 5/3 RIF (39/2012) (research excellence fund UiTM Malaysia) for financial support.

Appendix A. Supplementary data

Supplementary data related to this article can be found at http://dx.doi.org/10.1016/j.ejmech.2013.01.036.

References

[1] S. Dayawansa, K. Umeno, H. Takakura, E. Hori, E. Tabuchi, Y. Nagashima, H. Oosu, Yada, Y.T. Suzuki, T. Ono, H. Nishijo, Auton. Nerosci. 108 (2003) 79–86;
(a) G. Maatooq, S. El-Sharkawy, M.S. Afifi, J.P.N. Rosazza, J. Nat. Prod. 56 (1993) 1039–1050.
[2] K.C. Wang, L.Y. Ho, Y.S. Cheng, J. Chin. Biochem. Soc. 1 (1972) 53.
[3] V. Lamare, J.D. Fourneron, R. Furstoss, C. Ehret, B. Corbier, Tetrahedron Lett. 28 (1987) 6269–6272.
[4] J.R. Hanson, H. Nasir, Phytochemistry 33 (1993) 835–837.
[5] D.O. Collins, P.B. Reese, Phytochemistry 56 (2001) 417–421.
[6] W.R. Abraham, P. Washausen, K. Kieslich, Z. Naturforsch. 42C (1987) 414–419.
[7] Atta-ur-Rahman, M.I. Choudhary, F. Asif, A. Farooq, M. Yaqoob, A. Dar, Phytochemistry 49 (1998) 2341–2342.
[8] M.I. Choudhary, S. Sultan, M. Yaqoob, S.G. Musharraf, A. Yasin, F. Shaheen, Atta-ur-Rahman, Nat. Prod. Res. 17 (2003) 389–395.
[9] M.I. Choudhary, S. Sultan, M.T. Hassan, Atta-ur -Rahman, Steroids 70 (2005) 792–800.
[10] S.G. Musharraf, Atta-ur-Rahman, M.I. Choudhary, S. Sultan, Nat. Prod. Lett. 16 (2002) 345–349.
[11] M.I. Choudhary, Azizuddin, Atta-ur-Rahman, Nat. Prod. Lett. 16 (2002) 101–106.
[12] M.I. Choudhary, S. Sultan, S. Jalil, S. Anjum, A.A. Rahman, H.K. Fun, Atta-ur-Rahman, Chem. Biodivers. 2 (2005) 392–400.
[13] M.I. Choudhary, S. Sultan, M.T. Hassan, A. Yasin, F. Shaheen, Atta-ur-Rahman, Nat. Prod. Res. 18 (2004) 529–535.
[14] M.I. Choudhary, S.G. Musharraf, S.A. Nawaz, S. Anjum, M. Parvez, H.K. Fun, Atta-ur-Rahman, Bioorg. Med. Chem. 13 (2005) 1939–1944.
[15] M.I. Choudhary, S.G. Musharraf, A. Sami, Atta-ur-Rahman, Helv. Chim. Acta 87 (2004) 2685–2694.
[16] M.I. Choudhary, S.G. Musharraf, M.T.H. Khan, D. Abdaelrahman, M. Pervaz, F. Shaheen, Atta-ur-Rahman, Helv. Chim. Acta 86 (2003) 3450–3460.
[17] I.A. Sowthwell, A.J. Hayes, J.L. Markham, D.N. Leach, Acta Horticult. 334 (1993) 265–275.
[18] C. Braun, D.G. Brayers, G.W. Stephen, J. Biol. Chem. 270 (1995) 26778–26781.
[19] F. Shaheen, M. Ahmed, S.N. Han, S.S. Hussain, S. Anjum, B. Tashkhodjaev, K. Turgunov, M.N. Sultankhodzhaev, M.I. Choudhary, Atta-ur-Rahman, Eur. J. Org. Chem. 10 (2006) 2371–2377.
[20] M.W. Schmidt, K.K. Baldridge, J.A. Boatz, S.T. Elbert, M.S. Gordon, J.H. Jensen, S. Koseki, N. Matsunaga, K.A. Nguyen, S. Su, T.L. Windus, M. Dupuis, J.A. Montgomery, J. Comput. Chem. 14 (1993) 1347–1363.
[21] O. Trott, A.J. Olson, J. Comput. Chem. 31 (2010) 455–461.
[22] M.D. Hanwell, D.E. Curtis, D.C. Lonie, T. Vandermeersch, E. Zurek, G. R Hutchison, J. Cheminf. 4 (2012) 17.
[23] A.R. Allouche, J. Comput. Chem. 32 (2011) 174–182.
[24] W. Humphrey, A. Dalke, K. Schulten, J. Molec. Graphics 14 (1996) 33–38.
[25] E.F. Pettersen, T.D. Goddard, C.C. Huang, G.S. Couch, D.M. Greenblatt, E.C. Meng, T.E. Ferrin, J. Comput. Chem. 25 (2004) 1605–1612.
[26] R.V. Smith, J. Rosazza, J. Pharm. Sci. 64 (1975) 1737–1759.
[27] T. Matsui, C. Yoshimoto, K. Osajima, T. Oki, Y. Osajima, Biosci. Biotechnol. Biochem. 60 (1996) 2019–2022.